Surface-aligning field in smectic liquid-crystal films

LiDong Pan[1,2] and C. C. Huang[1]

[1]*School of Physics and Astronomy, University of Minnesota, Minneapolis, Minnesota 55455, USA*

[2]*Department of Physics and Astronomy, Johns Hopkins University, Baltimore, Maryland 21218, USA*

(Received 23 July 2011; revised manuscript received 20 October 2011; published 9 November 2011)

Two modified mean-field J_1-J_2 models are studied to explain the surface reduction of twisting power in the helical smectic-C^*_α phase in free-standing liquid crystal films. Profiles of the surface interlayer interaction are calculated from the experimental results. The calculations reveal the existence of a strong surface field and indicate that the surface field is the reason for the observed reduced twisting power near the surface region. Our results provide a quantitative study of the interlayer interactions through surface effects in smectic liquid crystals.

DOI: 10.1103/PhysRevE.84.051703 PACS number(s): 61.30.Hn, 64.60.an, 77.84.Nh

I. INTRODUCTION

The study of intermolecular interaction is very important for understanding the properties of materials. However, the direct experimental measurement of such interactions is usually a very challenging task. As a result, intermolecular interactions are often studied from indirect approaches; e.g., the strength of the ferromagnetic exchange interaction can be obtained from the value of the magnetic ordering temperature, when analyzed with appropriate models [1]. For soft materials, especially smectic liquid crystals, however, the situation is more complicated as several competing interactions are usually involved in the ordering and phase transitions [2].

Smectic liquid crystals have layered structures. Thus phase transitions between different smectic phases are usually driven by different types of interlayer interactions [2]. Although the understanding of those interactions are of great importance, so far very limited experimental studies on this topic have been published [3,4]. The lack of studies on interlayer interactions also hindered the theoretical advances of phase transitions in smectic liquid crystals, especially for the group of materials called antiferroelectric liquid crystals (AFLC) in which a total of six smectic-C^* (SmC^*, in which molecules are tilted away from the layer normal direction) variant phases are identified [5,6].

At the moment, one of the few quantitative studies of interlayer interactions in AFLC materials comes from the study of helical pitch of the smectic-C^*_α (SmC^*_α) phase [7]. In SmC^*_α, molecules are tilted away from the layer normal and the tilt direction of each layer is arranged in a helix along the layer normal, with pitch on the order of a few layers [8–10]. Since each smectic layer has a thickness of about 3 nm, SmC^*_α structure is optically uniaxial. The helical structure can be viewed as the result of the competition between nearest-neighbor (NN) interlayer interaction (J_1) and next-nearest-neighbor (NNN) antiferroelectric interlayer interaction (J_2). Thus, by analyzing the temperature evolution of the helical pitch in the J_1-J_2 model, a quantitative knowledge of the temperature evolution of J_1 and J_2 can be obtained [7].

On the other hand, in smectic liquid crystals, pronounced surface effects are usually observed, especially in film geometries [11]. The broken symmetry and surface tension at the air-liquid crystal interface create an array of interesting phenomena, including surface transitions [12–14], novel structures and/or transitions in thin films [15–17], layer by layer freezing or melting [18], and the recently observed surface reduction of twisting power in the SmC^*_α phase [19]. Although a detailed understanding of the surface interactions is yet to be achieved, some qualitative knowledge can be obtained.

In this paper we present a *quantitative* study of the interlayer interactions near the surface region in free-standing films of AFLC. Two modified J_1-J_2 models are proposed and used to explain the reduced twisting power in the SmC^*_α structure in free-standing films. Profiles of the interlayer interaction near the surface region are obtained from the calculation based on the experimental results reported in Ref. [19]. From the calculations, a strong surface aligning field is found to be the reason for the observed reduction of twisting power near the surface region in the SmC^*_α structure in free-standing films. These results provide new information and insights for both the study of surface effects in smectic liquid crystals as well as the study of interlayer interactions in AFLC materials. It also provides an example how the study of surface effects can facilitate our understanding of interlayer interactions in smectic liquid crystals.

II. EXPERIMENTAL RESULTS AND STRUCTURAL MODELS

In a recent paper, a null transmission ellipsometer was used to study the temperature evolution of the helical structures of the SmC^*_α phase in free-standing films of AFLC compound 10OTBBB1M7 [19]. The main experimental results are shown in the schematic illustrations of Fig. 1. In Fig. 1, the red arrow represents the tilt direction of the molecules in a given layer. The results showed reduced values of the rotation angle ϕ_i between the tilt directions of neighboring layers near the surface region (Fig. 1, right), where i is the distance from the biaxial surface layers. At each air-liquid crystal interface, there are several pretilted planar surface layers (N_S) that do not join in the formation of the helix. For the case of 10OTBBB1M7, $N_S = 3$ layers. It was found that the closer to the surface, the smaller ϕ_i will be. It was suggested that an enhanced aligning field due to the biaxial surfaces (Fig. 1, left) might be the reason for this phenomenon.

Two structural models (linear model and exponential model) were proposed to fit the data in Ref. [19]. Within experimental resolution, both models gave satisfactory results. In the linear model, a *buffer region* next to the surface layers

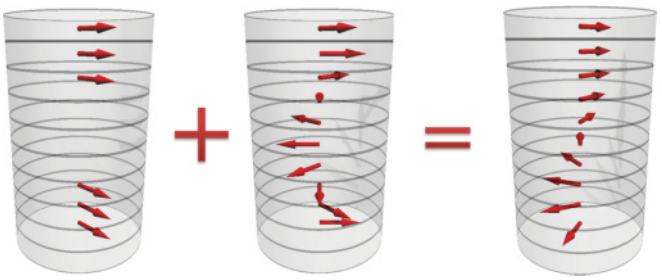

FIG. 1. (Color online) Schematic illustration of the main experimental result on the study of the SmC^*_α structure in free-standing films from Ref. [19]. Red arrows represent the tilt direction of each layer in the film. In the presence of biaxial surface ordered layers (left), the optically uniaxial SmC^*_α structure (middle) shows reduced twisting power (i.e., smaller rotation angle ϕ between the tilt direction of neighboring layers) near the surface region (right, top three layers are the biaxial surface layers).

with rotation angle ϕ_i smaller than the bulk value ϕ_b was assumed to have a size of a layers. In the buffer region, the rotation angle ϕ_i increases linearly as a function of the distance from the surface layers until it reaches the bulk value at a layers from the surface region. In the exponential model, on the other hand, the evolution of the rotation angle ϕ_i is given by an exponential function $\phi_b \times [1 - \exp(-i/\zeta)]$, with i being the distance from the biaxial surface region. In those models, a and ζ are the only fitting parameters, while the temperature evolution of ϕ_b of compound 10OTBBB1M7 has been obtained from previous resonant x-ray diffraction (RXRD) experiments.

Figure 2 shows the structural models described above for a film with 34 interior layers (excluding the biaxial surface layers). In the figure, size of the buffer region of the linear model $a = 6$ layers was used, while for the exponential model, $\zeta = 3$ layers. Those values are obtained from the best fit to the data given in Ref. [19]. A rotation angle equal to $\pi/3$, which corresponds to a pitch value of six layers, was used for the bulk value ϕ_b since for bulk 10OTBBB1M7, a pitch from about 5.5 to about 8.5 layers as a function of temperature was observed in previous RXRD studies. The main results discussed in the following text do not depend on the particular choice of pitch value.

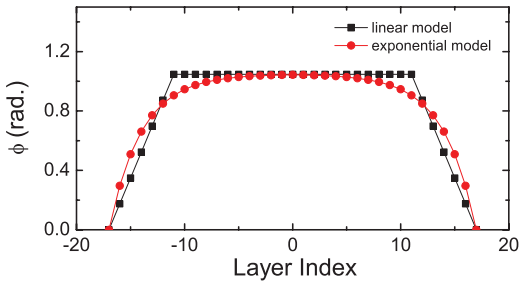

FIG. 2. (Color online) Profile of rotation angle ϕ as a function of position for a film with 34 interior layers from both the linear model (black squares) and the exponential model (red dots). In the linear model, a buffer region with size $a = 6$ layers was used, while in the exponential model, $\zeta = 3$ layers. For this figure, the bulk rotation angle $\phi_b = \pi/3$ was used, which corresponds to a pitch of six layers. The values of a and ζ were obtained from the fitting in Ref. [19].

The bulk helical structure of the SmC^*_α phase is understood as the result of the competition between the NN and the antiferroelectric NNN interlayer interactions. In the J_1-J_2 model, the corresponding free energy is given by

$$F = J_1 \sum \xi_i \cdot \xi_{i+1} + J_2 \sum \xi_i \cdot \xi_{i+2}. \quad (1)$$

Here ξ_i is a unit vector describing the tilt direction of the molecules in layer i, while J_1 and J_2 are the interaction coefficients. In the bulk, the rotation angle between neighboring layers is given by $\cos(\phi_b) = -J_1/4J_2$, with $|J_1/J_2| \leqslant 4$. For pitch greater than four layers, the NN interlayer interaction is of the ferroelectric type ($J_1 < 0$), as for the situation in 10OTBBB1M7.

Near the surface, there are fewer NNN bonds compared with NN bonds. Thus neighboring layers show a stronger tendency toward parallel alignment close to the surfaces [20,21]. However, the large size of the buffer region is intriguing; from the fitting it is twice the size of the biaxial surface. This suggests that a strong surface induced aligning field might be needed to produce the large buffer region observed in the experiment.

III. MEAN-FIELD MODELS

To gain further and more quantitative understanding, we studied those results in two modified J_1-J_2 models. The usual way of forming a theoretical understanding for experimental results would be through providing some format of trial interaction, and then calculating the corresponding set of rotation angles ϕ_i that minimizes the free energy. By comparing the calculated results to the experimental results, we would be able to gain some understanding of the driving forces of the reduced twisting power near the surface region.

Here we follow a different approach. Since from fitting the data to the structural models two sets of ϕ_i profiles are already obtained, it would be much more straightforward to obtain a corresponding profile of interaction coefficient from the ϕ_i profiles, provided proper phenomenological terms in the free-energy expression are included in the models.

First we add an anisotropy energy term to the J_1-J_2 model. This term has been shown to be essential for the formation of distorted clock structures in AFLC materials [22,23]. The free energy now reads

$$F = J_1 \sum \xi_i \cdot \xi_{i+1} + J_2 \sum \xi_i \cdot \xi_{i+2} + \sum b_i (\xi_i \times \xi_{i+1})^2, \quad (2)$$

where the b_i term is a position-dependent anisotropy energy that provides the necessary tendency toward planar alignment. The summation applies to all the interior layers. Thus the coefficient b_i is expected to be large near the surface and goes to zero in the interior of the film, where bulklike structures are observed.

The above equation can be rewritten in terms of ϕ_i as

$$F = J_1 \sum \cos(\phi_i) + J_2 \sum \cos(\phi_i + \phi_{i+1}) + \sum b_i [\sin(\phi_i)]^2. \quad (3)$$

For a film with N interior layers, we have $N - 1$ rotation angles ϕ_i between the neighboring layers. For the ground state

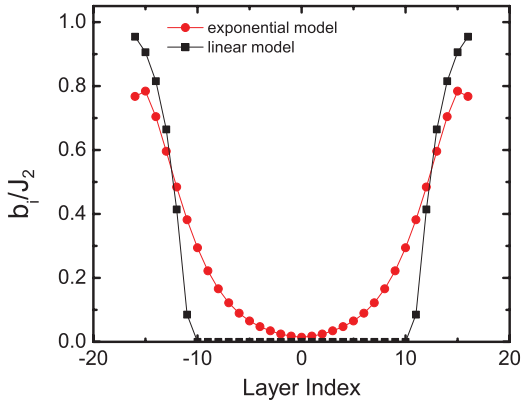

FIG. 3. (Color online) Calculated profile of the anisotropy interlayer interaction coefficient b_i/J_2 for a film with 34 interior layers. Results from both the linear model (black squares) and the exponential model (red dots) are shown. The rotation angle profile ϕ_i used in the calculation is obtained from Fig. 2, and $J_1 = -2J_2$ is used.

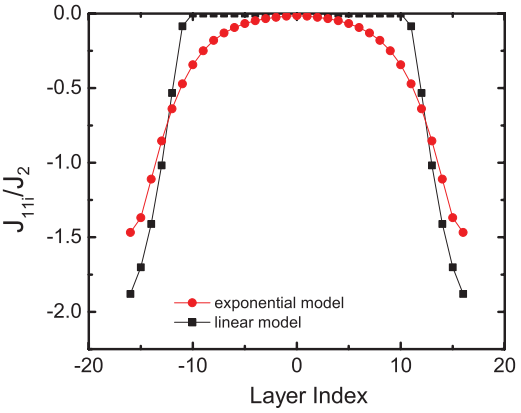

FIG. 4. (Color online) Calculated profile of the surface enhanced NN interlayer interaction coefficient J_{11i}/J_2 for a film with 34 interior layers. Results from both the linear model (black squares) and the exponential model (red dots) are shown. The rotation angle profile ϕ_i used in the calculation are obtained from Fig. 2, and $J_1 = -2J_2$ is used.

we expect to have $\partial F/\partial\phi_i = 0$ for all ϕ_i. Thus we would have $N-1$ equations for the system. From algebra, b_i/J_2 can be expressed as a function of ϕ_{i-1}, ϕ_i, ϕ_{i+1}, and J_1/J_2:

$$\frac{b_i}{J_2} = \left[\frac{J_1}{J_2}\sin(\phi_i) + \sin(\phi_{i-1}+\phi_i) + \sin(\phi_i+\phi_{i+1})\right] \Big/ \sin(2\phi_i). \tag{4}$$

From the J_1-J_2 model, we already know that in bulk systems $\cos(\phi_b) = -J_1/4J_2$. Thus given the profile of ϕ_i obtained from fitting the structural models, we are able to calculate the profile of anisotropy interlayer interaction b_i/J_2 that produces the observed ϕ_i.

Figure 3 shows the results of b_i/J_2 profile calculated from the ϕ_i profile shown in Fig. 2 for a film with 34 interior layers. Here b_i/J_2 for both the linear model and exponential model are shown. For the calculation, a bulk rotation angle of $\pi/3$ that corresponds to a $J_1 = -2J_2$ was used. The results show a large anisotropy coefficient near the surface region, as b_i/J_2 has its maximum value near the surface layers. The large values of b_i/J_2 near the surface region suggest the missing neighbor effect alone is incapable of producing the observed experimental results. Also, b_i/J_2 goes to zero in the center of the film as expected. Those results strengthen our argument that the observed reduction of twisting power near the surface region is indeed a surface effect. From the calculated b_i/J_2 profile we also find that range of this surface aligning field to be quite large. For the linear model it equals the size of the buffer region. However, for the exponential model, the range of finite b_i/J_2 is much larger (several times the size of ζ).

We also explored the possibility of an enhanced NN interlayer interaction near the surface region as the cause of the observed experimental results. Adding this term to the J_1-J_2 model instead of the anisotropy interaction, we would then have

$$F = J_1\sum \xi_i\cdot\xi_{i+1} + J_2\sum \xi_i\cdot\xi_{i+2} + \sum J_{11i}(\xi_i\cdot\xi_{i+1}) \tag{5}$$

and

$$F = J_1\sum\cos(\phi_i) + J_2\sum\cos(\phi_i+\phi_{i+1}) + \sum J_{11i}\cos(\phi_i). \tag{6}$$

Here J_{11i} is a position-dependent NN term that is expected to reach zero deep in the center of the film. It provides the necessary enhanced tendency toward parallel alignment near the surface region. Following the same procedure as described above, now we have

$$\frac{J_{11i}}{J_2} = -\frac{J_1}{J_2} - [\sin(\phi_{i-1}+\phi_i) + \sin(\phi_i+\phi_{i+1})]/\sin(\phi_i). \tag{7}$$

From the calculation, we obtained a J_{11i}/J_2 profile as shown in Fig. 4.

From Fig. 4 we find that J_{11i}/J_2 goes to zero in the center of the film as expected. However, the large increase of its magnitude near the surface region and the large range of interaction suggest a really strong enhancement of the NN interlayer interaction near the surface, if we do not consider the anisotropy interaction. Note $J_{11i}+J_1$ is the total NN interlayer interaction, and since we have $J_1 = -2J_2$ for this calculation, about a 100% (about 80%) enhancement is found in the calculated results for the linear (exponential) model near the surface.

IV. DISCUSSION AND CONCLUSION

From those calculations, it is clear that the reduced twisting power near the surface region is indeed the result of a strong surface interlayer interaction, which has a large effective range. The phenomenological origins of those surface enhanced interlayer interactions [b_i and J_{11i} terms in Eqs. (3) and (5)] can be understood in the framework of the Landau models of surface transitions in smectic films [24–26]. In the Landau models, enhanced surface order is introduced through increased transition temperatures of the surface layers. This leads to increased values of the order parameter (tilt angle) near

surface layers in the ordered phase and results in the increased values of the interlayer interaction terms b_i (which describes the energy barrier between synclinic and anticlinic ordering) or the enhanced NN term J_{11i}. Following this reasoning, the change of these interactions as a function of layer position (as well as the effective ranges) can also be understood under the Landau models with a finite surface correlation length.

On the other hand, the microscopic origin of this surface interlayer interaction is beyond our phenomenological treatment. However, the biaxial planar surface layers are expected to have larger values of tilt angles, while the fluctuations near the surface layers are suppressed due to the presence of surface tension. Thus it is possible the surface interlayer interaction revealed in our calculation resulted from the fluctuation induced interlayer interactions and/or the anisotropy elastic constants of tilted smectic layers [27–29].

Here we would like to point out that the only assumption made in our calculation is the choice of the surface enhanced interlayer interaction term. All the numerical values used came directly from experiments. Results from the two situations (anisotropic interlayer interaction or surface enhanced NN interlayer interaction) yield qualitatively the same behavior for the surface field profile. They show maximum values near the surface region and reach zero deep in the interior of the film. This indicates that our conclusion does not depend on the choice of phenomenological terms. In our study we did not attempt a model with both the anisotropic interaction and the enhanced NN interaction to avoid introducing too many free parameters. There is also no reason that the calculated enhanced surface interlayer interaction should be restricted to compound 10OTBBB1M7 or the SmC^*_α phase only. Thus our results also serve as a quantitative study of the interlayer interaction as well as surface effects in smectic liquid crystals.

In summary, we studied the reduced twisting power near the surface region in the helical SmC^*_α phase of free-standing films in two modified J_1-J_2 models. An anisotropy interlayer interaction or an enhanced surface NN interlayer interaction term was added to the original free-energy expression. Strong surface interlayer interactions were found to be the reason for this phenomenon. Profiles of the surface interlayer interactions are calculated from the structures obtained from fitting the experimental data. The effective ranges of the surface fields are found to be very large.

This study presents a unique example of studying the interlayer interaction through the investigation of surface effects in smectic liquid crystals. Given the common occurrence and rich variety of surface effects in smectic liquid crystals, our approach provides an excellent alternative route for studying the interlayer interactions in smectic liquid crystals.

ACKNOWLEDGMENT

This research was supported in part by the National Science Foundation, Solid State Chemistry Program, under Grant No. DMR-0605760.

[1] L. J. de Jongh and A. R. Miedema, Adv. Phys. **23**, 1 (1974).
[2] P. G. de Gennes and J. Prost, *The Physics of Liquid Crystals*, 2nd ed. (Oxford University Press, New York, 1995).
[3] L. Moreau, P. Richetti, and P. Barois, Phys. Rev. Lett. **73**, 3556 (1994).
[4] P. V. Dolganov, P. Cluzeau, G. Joly, V. K. Dolganov, and H. T. Nguyen, Phys. Rev. E **72**, 031713 (2005).
[5] H. Takezoe, E. Gorecka, and M. Čepič, Rev. Mod. Phys. **82**, 897 (2010).
[6] S. Wang, L. D. Pan, R. Pindak, Z. Q. Liu, H. T. Nguyen, and C. C. Huang, Phys. Rev. Lett. **104**, 027801 (2010).
[7] A. Cady, D. A. Olson, X. F. Han, H. T. Nguyen, and C. C. Huang, Phys. Rev. E **65**, 030701 (2002).
[8] P. Mach, R. Pindak, A.-M. Levelut, P. Barois, H. T. Nguyen, C. C. Huang, and L. Furenlid, Phys. Rev. Lett. **81**, 1015 (1998).
[9] D. Schlauf, C. Bahr, and H. T. Nguyen, Phys. Rev. E **60**, 6816 (1999).
[10] P. M. Johnson, S. Pankratz, P. Mach, H. T. Nguyen, and C. C. Huang, Phys. Rev. Lett. **83**, 4073 (1999).
[11] W. H. de Jeu, B. I. Ostrovskii, and A. N. Shalaginov, Rev. Mod. Phys. **75**, 181 (2003).
[12] L. D. Pan, S. Wang, C. S. Hsu, and C. C. Huang, Phys. Rev. E **79**, 031704 (2009).
[13] L. D. Pan, B. K. McCoy, S. Wang, W. Weissflog, and C. C. Huang, Phys. Rev. Lett. **105**, 117802 (2010).
[14] C. Y. Chao, T. C. Pan, and J. T. Ho, Phys. Rev. E **67**, 040702 (2003).
[15] C. Bahr and D. Fliegner, Phys. Rev. Lett. **70**, 1842 (1993).
[16] D. Schlauf and C. Bahr, Phys. Rev. E **57**, 1235 (1998).
[17] P. V. Dolganov, Y. Suzuki, and A. Fukuda, Phys. Rev. E **65**, 031702 (2002).
[18] T. Stoebe, P. Mach, and C. C. Huang, Phys. Rev. Lett. **73**, 1384 (1994)
[19] L. D. Pan and C. C. Huang, Phys. Rev. E **83**, 060702 (2011).
[20] E. Weschke, H. Ott, E. Schierle, C. Schüssler-Langeheine, D. V. Vyalikh, G. Kaindl, V. Leiner, M. Ay, T. Schmitte, H. Zabel, and P. J. Jensen, Phys. Rev. Lett. **93**, 157204 (2004).
[21] L. D. Pan, S. Wang, C. S. Hsu, and C. C. Huang, Phys. Rev. Lett. **103**, 187802 (2009).
[22] Mojca Čepič and Boštjan Žekš, Phys. Rev. Lett. **87**, 085501 (2001).
[23] D. A. Olson, X. F. Han, A. Cady, and C. C. Huang, Phys. Rev. E **66**, 021702 (2002).
[24] S. Heinekamp, R. A. Pelcovits, E. Fontes, E. Y. Chen, R. Pindak, and R. B. Meyer, Phys. Rev. Lett. **52**, 1017 (1984).
[25] P. V. Dolganov, V. M. Zhilin, V. K. Dolganov, and E. I. Kats, Phys. Rev. E **67**, 041716 (2003).
[26] N. Vaupotic and M. Čepič, Phys. Rev. E **71**, 041701 (2005).
[27] M. B. Hamaneh and P. L. Taylor, Phys. Rev. Lett. **93**, 167801 (2004).
[28] M. B. Hamaneh and P. L. Taylor, Phys. Rev. E **72**, 021706 (2005).
[29] R. Bruinsma and J. Prost, J. Phys. II France **4**, 1209 (1994).